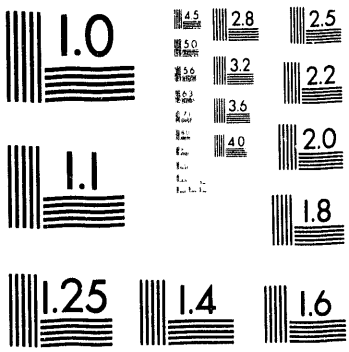
1.0
1.1
1.25
1.4
1.6
1.8
2.0
2.2
2.5
2.8
3.2
3.6
4.0
4.5
5.0
5.6

1 of 1

Conf-9306223--2

LBL-34763
UC-404

Lawrence Berkeley Laboratory
UNIVERSITY OF CALIFORNIA

Materials Sciences Division

Presented at the NATO ASI on Nanophase Materials:
Synthesis-Processes-Applications, Corfu, Greece,
June 24–July 10, 1993, and to be published in the Proceedings

SE EXAFS Study of the Elevated Wurtzite to Rock Salt Structural Phase Transition in CDSE Nanocrystals

S.H. Tolbert and A.P. Alivisatos

September 1993

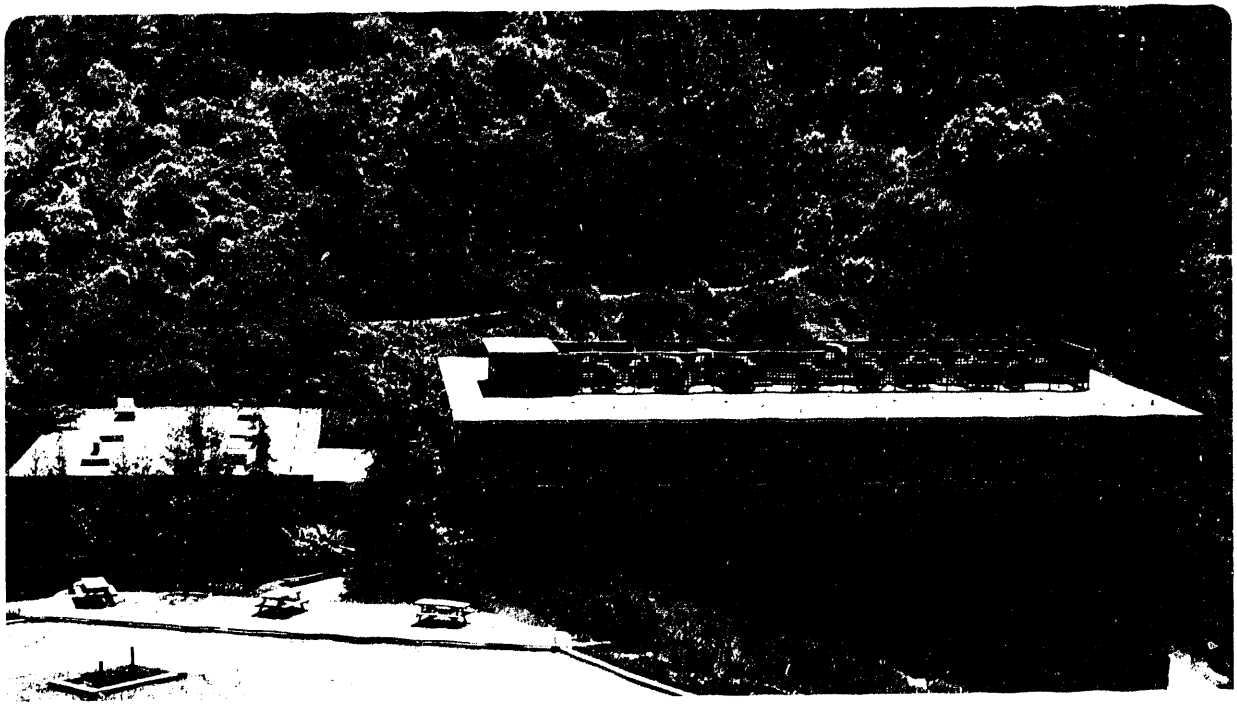

Prepared for the U.S. Department of Energy under Contract Number DE-AC03-76SF00098

DISCLAIMER

SE EXAFS STUDY OF THE ELEVATED WURTZITE TO ROCK SALT STRUCTURAL PHASE TRANSITION IN CDSE NANOCRYSTALS

S. H. TOLBERT and A. P. ALIVISATOS
Materials Sciences Division
Lawrence Berkeley Laboratory
and
Department of Chemistry
University of California
Berkeley, California 94720, U.S.A.

ABSTRACT. High pressure Se EXAFS data has been obtain on 2.7 nm radius CdSe semiconductor nanocrystals. This system is observed to undergo a solid-solid phase transition at 6.5 GPa which is approximately twice the reported value for bulk CdSe. In combination with high pressure optical absorption experiments, EXAFS data can be used to identify the high pressure phase structure as rock salt. EXAFS data can be fit with equations of state to yield pressure volume curves. The resultant values of the bulk modulus and its derivative with respect to pressure are B_o = 37 ± 5 GPa and B_o' = 11 ± 3. A thermodynamic model for the data is presented in which the internal energy in each phase is modified by a surface energy term. Differences in surface energy are used to explain the elevation in phase transition pressure. The model can be used to estimate a value for the surface energy in the rock salt phase. A value of 1.9 ± 0.3 N/m is obtained in comparison to 0.9 ± 0.1 N/m for the wurtzite phase.

1. Introduction

How will the phase transition from one solid structure to another be different in a nanocrystal, as compared to the bulk sold? As the domain size of a material is decreased, how will this effect the relative stability of different possible structures of the material? This question has ramifications in fields as diverse as electrical engineering, where the size of features in integrated circuits is approaching the nm regime, and geo-physics, where the phase diagram of solids with nanometer domain sizes is unknown. Changes in phase transition points with the intrinsic size of a nanocrystal may arise through the influence of the surface of the nanocrystals, which adds a large term to the internal energy of each phase, or potentially through purely dynamical effects, since the length scale of the maximum possible fluctuation in a nanocrystal is restricted by its size. In this paper we present a structural study of the pressure induced transformation from a dominantly covalent, four-coordinate wurtzite structure to an ionic six coordinate rocksalt structure in a sample containing nanocrystals of CdSe homogeneously dispersed in a pressure transmitting medium.

This work has been partially supported by the donors of the Petroleum Research Fund, administered by the American Chemical Society; and by the Director, Office of Energy Research, Office of Basic Energy Sciences, Materials Sciences Division, of the U.S. Department of Energy under Contract No. DE-AC03-76SF00098.

Recent developments in synthetic methods now allow for the preparation of crystalline, highly monodisperse CdSe nanocrystals in a wide range of sizes. In addition, recent high pressure studies on CdS[1,2] and CdSe[3,4] nanocrystals have shown surprising results. While both of these bulk systems undergo a high pressure phase transition from a low pressure covalent phase to a high pressure rock salt phase at about 3 GPa[5,6,7], experiments using optical absorption and resonance Raman spectroscopies show that for nanocrystals in the 2-5 nm range, the covalent phase is stable to pressures 2-3 times those observed in bulk systems. Due to the indirect nature of the high pressure phase band gap however, no information on the high pressure phase structure can be obtained from these experiments. Similar experiments on GaAs/AlAs multilayers[8] also show an elevation in phase transition pressure, though again high pressure phase structures can only be speculated on by analogy with bulk systems.

A related question to the effect of finite size on high pressure transitions is the well known reduction of the melting temperature in nanocrystals. Much progress has been made in understanding these transitions. In a wide variety of materials, ranging from metals[9,10] to semiconductors[11], changes in melting temperature with size can be almost completely accounted for by a thermodynamic model in which the surface energy of the liquid phase is less than that of the solid. For nanometer size particles, essentially no hysteresis is observed in the melting curves; that fact, coupled with the at least qualitative success of the thermodynamic surface energy model, leads to the conclusion that dynamical effects play no role in the reduction of melting temperature. The same may not hold true for solid-solid phase transitions at room temperature, where substantial barriers must be overcome, and large hysteresis effects are sometimes observed even in the bulk material. A detailed knowledge of the structural changes with pressure in a nanocrystal system are needed to see whether thermodynamic or kinetic effects predominate.

The goal of this experiment is thus to obtain direct structural data on nanocrystalline systems at high pressure. The two direct structural techniques that can be applied to characterize the system are X-ray diffraction and EXAFS. We have chosen to start with Se EXAFS because of the intrinsic lack of long range order in nanocrystals. While we have subsequently shown that it is possible to obtain complementary diffraction data on the nanocrystals at high pressure, EXAFS provides a direct measure of the Cd-Se bond length and as such is ideally suited for our purpose. In order to apply thermodynamics to these systems, we require the pressure-volume curves. It should be noted that the goal of this experiment is only to obtain data on the Cd-Se bond length. While EXAFS is frequently reported to accurately measure both the coordination number and the bond length, the coordination number data is generally not as certain, and this is even more so for EXAFS measurements performed on samples in a diamond anvil cell. The period of the EXAFS oscillations arises from the size of the reflecting cavity that surrounds the absorbing atom, and is unaffected by the cell. Changes in the coordination number will result in a change in the total amplitude of the oscillation relative to the absorption edge. This amplitude can be perturbed by background from the high pressure cell. In addition, the amplitude of the oscillations is a function of both the coordination number and the Debye-Waller factor in the material, and these two effects are very hard to separate. As

the pressure of the system is increased the Debye-Waller factor is constantly changing, and these changes tend to manifest themselves as anomalous change in coordination number. Because of all of these effects, we will only report bond length data for high pressure samples. This is sufficient information however to calculate the required constants to test the ideas of surface thermodynamic in understanding this elevated phase transition pressure.

A size dependence to the phase transition pressure arises in the thermodynamic formalism as follows. For bulk systems, the internal energy for the high and low pressure phases are given by:

$$\begin{aligned} U_1(T,P) &= TS_1(T,P) - PV_1 + \mu_1 N_1 \\ U_2(T,P) &= TS_2(T,P) - PV_2 + \mu_2 N_2 \end{aligned} \qquad (1)$$

where U, S, and μ are the internal energy, the entropy, and the chemical potential, respectively for each phase. The condition for a phase transition to occur is $\mu_1 = \mu_2$. As the temperature dependence of these solid-solid phase transitions is weak, and the entropy change at the phase transition is small, it is customary to ignore the TS_i terms in equation 1 when calculating thermodynamic parameters from experimental data. In the case of a nanocrystalline system, equation 1 must be modified by a surface energy term:

$$\begin{aligned} U_1(P,V) &= TS_1 - PV_1 + \mu N_1 - \gamma_1 A_1 \\ U_2(P,V) &= TS_2 - PV_2 + \mu N_2 - \gamma_2 A_2 \end{aligned} \qquad (2)$$

where γ_i and A_i are the surface tension and surface area respectively in phase i. The elevation in phase transition pressure can be expected if $\gamma_{\text{rock salt}}$ is greater than γ_{wurtzite}.

With a knowledge of the structural changes in isolated nanocrystals of CdSe under pressure, these thermodynamic equations can be applied both to model the data, and extract extract the surface energies. To this end, we have obtained high pressure Se EXAFS data on 2.7 nm radius CdSe nanocrystals. We will use this data to apply the ideas of surface thermodynamics to understanding the elevated phase transition pressure in these systems.

2. Experimental

The CdSe nanocrystals used in this experiment were prepared chemically using a modification of the method of Murray and Bawendi[12]. Crystallites were characterized using X-ray powder diffraction, TEM, optical absorption, and Raman scattering. Crystallite size and size distribution were determined using TEM and Small Angle X-ray Scattering (SAXS). The sample used in this experiment was found to be wurtzite in structure with an average size of 2.7 nm radius with a $\sigma$of 18%. Imperfect agreement between SAXS/TEM sizes and X-ray domain size indicates the presence of some stacking

faults or grain boundaries in the sample.

High pressure optical absorption data was obtained using a scanning Cary model 118 UV/visible spectrometer in combination with a Mao-Bell type diamond anvil cell with spring steel gaskets and 0.2 mm diameter sample chambers. Nanocrystals were dissolved in 4-ethyl-pyridine, a solvent which has been shown to be a good hydrostatic pressure medium to pressures in excess of 10 GPa. Pressure was determined using ruby fluorescence. In all cases, multiple fluorescence measurements were taken at various locations in the cell and pressure gradients were shown not to exceed 8%.

Se EXAFS data was obtained at the Stanford Synchrotron Radiation Laboratory on focused wiggler beam lines 6-2 and 10-2. Atmospheric pressure data was obtained using X-ray fluorescence and a Lytel detector. High pressure data was obtained in an absorption geometry using ion chamber detectors.

A significant problem with high pressure EXAFS experiments is interference due to Bragg diffraction from the single crystal diamonds of the high pressure cell. This diffraction can cause a forest of peaks that completely obscure the structure in the EXAFS region. Some improvement can be made by rotating the cell around its azimuthal angle. As a result of small imperfections in the diamond cutting, this moves the diffraction peaks in energy away from the region of interest and allows for empirical optimization of the EXAFS spectra. This technique is limited however, by the fact that the orientation of the two diamonds with respect to each other is fixed in the process of aligning the cell, and thus complete optimization is not possible. Other methods of dealing with interfering bragg diffractions includes replacement of the diamond anvils with Boron Carbide (B_4C) anvils[13]. Boron Carbide is polycrystalline, and thus produces no interfering diffraction peaks. It has the limitation that it is not optically transparent and thus precludes the use of ruby fluorescence to determine pressure. We have thus chosen to conduct our experiments using a modified Merrill-Bassett type diamond anvil cell with one diamond anvil, and one B_4C

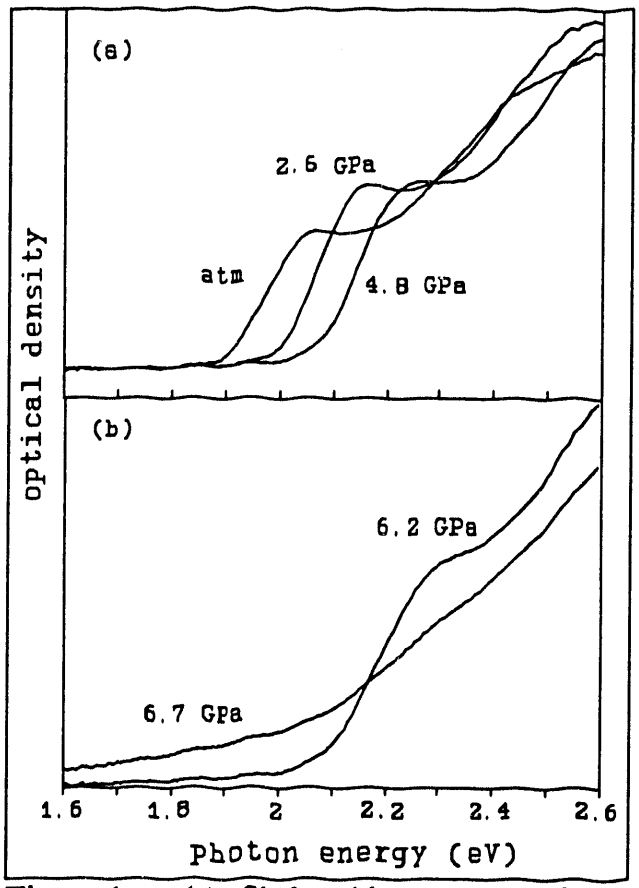

Figure 1: (a) Shift with pressure of the quantum confined optical absorption peak of 2.7 nm radius CdSe nanocrystal. (b) Disappearance of the confined feature at the structural phase transition pressure.

anvil. This allows for complete rotational optimization of the single diamond as well as providing an optical window for ruby fluorescence measurements.

EXAFS data was analyzed using standard procedures[14]. Data was background corrected, Fourier filtered, and fit to a standard EXAFS equation:

$$\chi(k)=\frac{N}{k\cdot r^2}e^{-2\sigma^2k^2}\cdot F(k)\cdot\sin[2kr+\phi(k)] \qquad (3)$$

where k is the photoelectron wavevector, N is the number of nearest neighbors, r is the real space bond length, σ is the Debye-Waller factor, F(k) is the backscattering amplitude, and Φ(k) is the total phase shift experienced by the photoelectron. Scattering phase and amplitude factors were calculated theoretically using bulk CdSe lattice geometry in combination with the program Feff 5, version 5.04.

3. Results

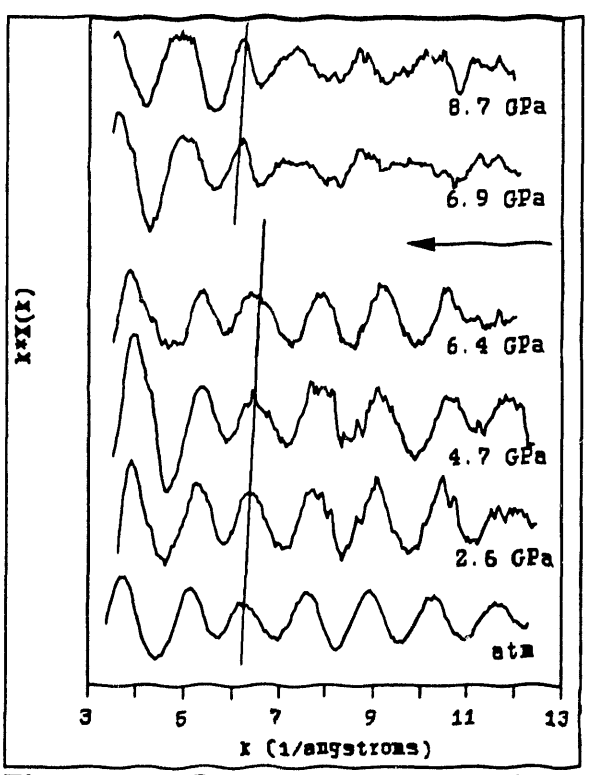

Figure 2: Back ground corrected Se EXAFS data, k*X(k), obtained for CdSe nanocrystals as a function of pressure. The arrow corresponds to the optically detected phase transition point.

Optical absorption spectra of these direct gap semiconductors nanocrystals show a discrete absorption feature at energies above the bulk band gap due to quantum confinement of the initial electronic excited state. This feature is seen to move smoothly to higher energy upon the application of pressure. At pressures between 6.2 and 6.7 GPa, approximately 2 times the reported bulk transition pressure, the discrete feature disappears and is replaced by a weak featureless absorption, shifted to the red of the direct gap feature (figure 1). Upon release of pressure, the discrete absorption is recovered, though the reverse transition is marked by hysteresis.

Se EXAFS data on atmospheric pressure nanocrystal samples produces a bond length of 2.61 (Å) and a coordination number of 3.5, in good agreement with bulk CdSe values of 2.62 (Å) and 4. Raw EXAFS data obtained on our nanocrystal samples at a variety of pressures is presented in figure 2. The data shifts monotonically upon the

application of pressure up to 6.4 GPa, at which point a discontinuous change is observed, followed by another smooth shift. Cadmium-Selenium bond length changes obtained form fitting this data are presented in figure 3. The CdSe bulk linear compressibility is included for comparison. Data obtained upon the gradual release of pressure (5.5, 2.5 and 0.7 GPa) appears to show a mixed phase with a very low coordination number and a poorly defined bond length, though the 5.5 GPa data does appear to be dominantly rock salt in character. Upon full release of pressure, the bond length is observed to return to 2.63 (Å) and the coordination number to 3.4.

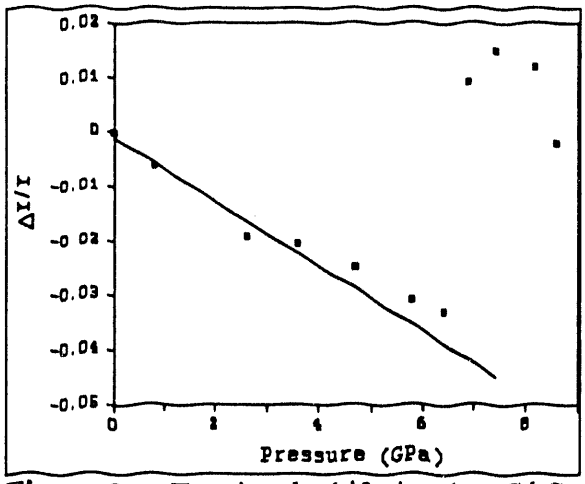

Figure 3: Fractional shift in the Cd-Se bond length with pressure for CdSe nanocrystals obtained from Se EXAFS. The line represents the bulk CdSe linear compressibility of 0.00593 GPa^{-1}.

4. Discussion

4.1. INTERPRETATION OF STRUCTURAL DATA

Optical absorption data suggests that 27 Å radius CdSe nanocrystals undergo a reversible solid-solid phase transition at pressures between 6.2 and 6.7 GPa. Roughly parabolic energy dependence in the high pressure phase absorption spectra further suggests that this new phase has an indirect band gap[15]. By analogy with the bulk, a reasonable structural candidate is rock salt, though other distorted octahedral structures with multiple first shell bond lengths are possible[16]. Other possibilities include amorphous or disordered states. Although it is not possible to distinguish between these possibilities using optical absorption, EXAFS can clearly separate the two. Amorphous material should show a distribution of bond lengths and a low average coordination number. In contrast, rock salt material should show a single peak when the back ground subtracted data is Fourier transformed into real space. Other six coordinate structures would show multiple prominent bond lengths.

Figure 4 shows that good quality EXAFS data can be obtained on high pressure phase nanocrystals, and that the EXAFS spectrum is dominated by a single bond length. These data suggest that the high pressure phase is not amorphous, and that the structure has only one dominant bond length. A small Se-Se second shell peak further suggests that the high pressure phase material has some degree of long range order. Although this is not sufficient information to positively identify the high pressure phase structure as rock salt, additional information can be gained by considering bond lengths. Figure 3 shows the fractional change in bond length with pressure. At the optically detected phase transition point, the bond length is observed to become suddenly longer. This is indicative of a

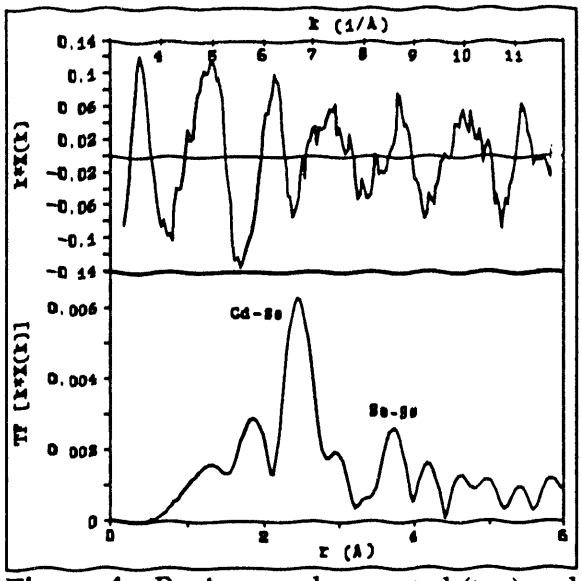

Figure 4: Back ground corrected (top) and Fourier transformed (bottom) Se EXAFS data obtained on CdSe nanocrystals at 8.2 GPa in the rock salt phase. Cd-Se and Se-Se shell peaks are indicated in the transformed spectra.

transition to a structure with a higher coordination number and packing fraction. The only reasonable structure that fills all of these requirements is rock salt. In addition, high pressure X-ray powder diffraction just obtained on these systems positively confirms the structural identity of the high pressure phase as rock salt.

With a knowledge of the high and low pressure phase structure, it becomes possible to calculate the volume change upon transition. Studies on a wide variety of materials show that wurtzite or zinc blende to rock salt transitions are usually accompanied by about a 20% decrease in unit cell volume[17,18]. Figure 5 shows the actual data for our 27 Å clusters. A 24% volume contraction is observed.

Complete recovery of the four coordinate structure by atmospheric pressure is supported by both optical absorption and EXAFS data. Optical absorption shows a return of the discrete, allowed band gap transition in atmospheric pressure recovered samples, and EXAFS shows a bond length and coordination number in atmospheric pressure recovered samples that is in good agreement with unpressurized samples. At pressures however, only slightly above atmospheric (less than 1 GPa), both EXAFS and optical absorption show incomplete recovery of the wurtzite phase. Although this type of solid-solid transition usually exhibits large hysteresis, our nanocrystals appear to show significantly more hysteresis than bulk CdSe[5]. This is a subject of current investigation.

4.2. CALCULATION OF THERMODYNAMIC PARAMETERS

The data presented in figure 5 can be fit with the Murnaghan equations of state[19]

$$V = \frac{V_o}{\left(1 + \frac{B_o'}{B_o} \cdot P\right)^{\frac{1}{B_o'}}} \qquad (4)$$

to yield values of B_o (the bulk modulus) and its derivative with respect to pressure (B_o'). B_o is the reciprocal of the linear volume compressibility. Most B_o values for covalent semiconductors are in the range of 50-100 GPa, with B_o' small, on the order of 1. The values obtained for our CdSe nanocrystals show $B_o = 37 \pm 5$ GPa and $B_o' = 11 \pm 3$. This

can be understood by noting that the compressibility of the CdSe nanocrystals seems to decrease at extremely high pressure. In bulk systems where this part of P-V space in not accessible, compressibility data can only be fit to the region between atmospheric pressure and 3 GPa. The nanocrystal data in that low pressure region is quite linear and can be accurately fit using bulk values of B_o. As the system is compressed beyond the bulk stability limit, we begin to sample the anharmonic parts of the Cd-Se potential and the compressibility deviates from the bulk value. The anomalous high pressure stability of these systems thus allows us to better determine the anharmonic terms in the potential of both the nanocrystals and the bulk.

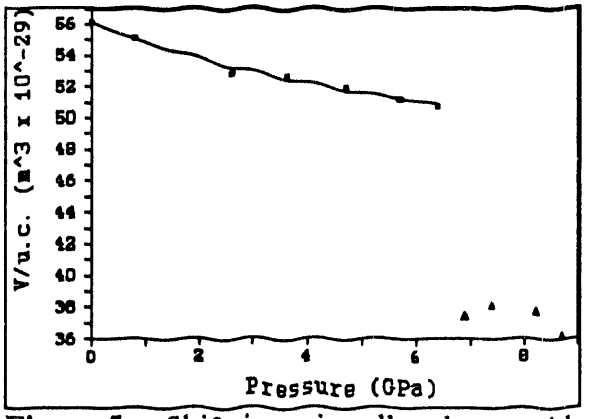

Figure 5: Shift in unit cell volume with pressure for 2.7 nm CdSe nanocrystals. The data is calculated from figure 2. The line represents a fit to the Murnaghan equations of state (equation 4).

While the high pressure phase data presented here is not sufficient to fit with a compressibility value, it can be used in combination with bulk high pressure phase diffraction data to obtain a reasonable value for the rock salt phase linear compressibility. It should be noted though that it is not strictly legitimate to use bulk and nanocrystal data together in this way, as the nanocrystal bond lengths should be shifted to slightly smaller bond lengths due to the effects of surface tension. These lattice contraction effects however are small in comparison to pressure induced bond length changes and so the error introduced by this method of calculation is not unreasonable. From our rock salt phase EXAFS data and the data of Mariano and Warekois[20], we calculate a B_o value of 66.3 GPa with an atmospheric pressure unit cell volume of 4.40×10^{-29} m^3. These values will prove useful in the following section. While the quality of the data is not sufficient to obtain a B_o' value, it can be assumed that this value will be small as the pressures reached in this experiment are much lower than any reported second phase transitions observed in bulk CdSe. In the rock salt phase, the system is probably still in the harmonic part of the Cd-Se potential.

4.3. A THERMODYNAMIC MODEL FOR THE PHASE TRANSITION

With a knowledge of all of the thermodynamic constants of the system, we are now in a position to apply the ideas and equations of surface thermodynamics to this solid-solid phase transition. The chemical potentials in equation 2 can be equated and the entropy terms discarded to produce

$$P_T(V_1-V_2)+U_1(P_T)-U_2(P_T)=\gamma_2 A_2+\gamma_1 A_1 \qquad (5)$$

where P_T is the phase transition pressure. While the value of $U_1(P_T)$-$U_2(P_T)$ itself is not

known, it can be calculated from known quantities. By equating the chemical potentials in equation 1, it is possible to obtain the expression

$$U_1(P_B) - U_2(P_B) = -P_B(V_1 - V_2) \tag{6}$$

where P_B is the bulk phase transition pressure of 3.0 GPa. As the changes in U with pressure can be calculated by integrating the pressure volume curves for each phase, equation 5 can now be rewritten as

$$(P_T - P_B)\cdot(V_1 - V_2) - \int_{P_B}^{P_T} P dV_1 + \int_{P_B}^{P_T} P dV_2 = \gamma_2 A_2 + \gamma_1 A_1 . \tag{7}$$

Note that this equation assumes that (V_1-V_2) is the same for both the bulk and nanocrystal phase transition. This assumption is reasonable and can be explicitly corrected for if more accurate values are required.

A more detailed discussion of the terms in equation 7 is perhaps in order. The first term is a measure of the additional PdV work that is required to make the system undergo a phase transition in the nanocrystals as compared to the bulk. The extra work manifests itself in the fact that for the nanocrystals, the volume contraction at the phase transition is taking place at a higher pressure. This work is required to overcome the additional surface energy of the high pressure phase, relative to the low pressure phase. The next two terms are modifications of the first term. They say that it is not correct to simply calculate the additional PdV work because there is also energy stored in the lattice and that amount of energy is not the same in wurtize and rock salt phases. One must modify the PdV work by the difference in the energy stored in the high and low pressure phase lattices. The stored energy can be calculated by integrating the equation of state. The integrated forms for the case where B_o' is and is not known are presented in equations 8 and 9 respectively.

$$E(V) = -\int P dV = \frac{B_o}{B_o'} V \left[1 + \left(\frac{(V_o/V)^{B_o'}}{(B_o' - 1)} \right) \right] + cnst \tag{8}$$

$$E(V) = -\int P dV = B_o V - B_o V_o \cdot \ln(V) + cnst \tag{9}$$

The final term says that all of this extra work needs to be equated to the difference in surface energy between the high and low pressure phases.

A value of the wurtzite phase surface energy can be experimentally determined from atmospheric pressure X-ray diffraction data on a variety of nanocrystal sizes. The data is presented in figure 6 and shows a decrease in d spacing with decreasing crystallite size. The Laplace Law (equation 10) relates this lattice contraction to an effective surface pressure (P_s) which can in tern be related to the cluster surface to volume ratio and a

single effective surface tension for the cluster.

$$P_S = \frac{2 \cdot \gamma}{r} \qquad (10)$$

A more accurate description of the surface tension would require an exact knowledge of crystallite shape and the energies of all of the surface planes present. The value obtained from multiple sizes of CdSe with the same chemical passivation on the surface is γ = 0.9 ± 0.1 N/m. The various points in figure 6 at each size represent the fractional shift in the (110), the (112), and the (103) diffraction peaks.

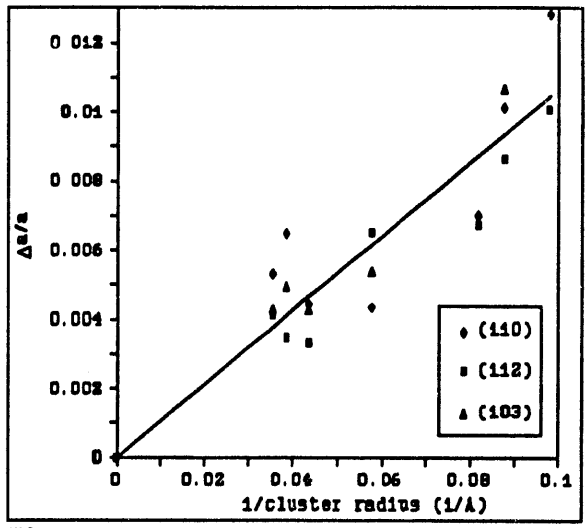

Figure 6: Fractional change in bond length with CdSe nanocrystal size. The line represents a best fit to the data. Different symbols indicate various diffraction peaks in the wurtzite X-ray powder pattern.

Although the purpose of this thermodynamic discussion is to better understand the elevation in the phase transition pressure in these nanocrystalline systems, an added benefit is that we now have sufficient information to calculate a value for the surface tension in the high pressure phase. As all of the terms of equation 7 are known except γ_2; we can solve for this value. The result is $\gamma_{\text{rock salt}}$ = 1.9 ± 0.3 N/m. While this value is quite high for a rock salt phase surface energy, it is not unreasonable in consideration of the fact that the high pressure phase surface is not formed to minimize high energy structures like edges and corners. Its formation is instead dictated by the microscopic path that the atoms must travel along to move from the wurtzite structure to the rock salt structure. Preliminary calculations suggest that this path may produce many very high energy surfaces.

4.4. IMPLICATIONS AND FUTURE WORK

Although this thermodynamic construction is not proven by the argument presented here, it is fully consistent with the data, and it is possible to further test it. The values in equation 7 all contain (or can be made to contain) only the variables P_T and the nanocrystal radius r, with $\gamma_{\text{rock salt}}$ the only unknown constant. This data can then be fit to phase transition data on a variety of nanocrystal sizes to see if a single value of $\gamma_{\text{rock salt}}$ is sufficient to describe all sizes. High pressure optical absorption data on a variety of sizes shows a monotonic decrease in phase transition pressure with increasing nanocrystal size. Work is currently underway to fit this data with the above thermodynamic equations.

The implications of this work to fields outside of solid state physics and chemistry are interesting and merit some speculation. Although these experiments were performed on isolated nanocrystals homogeneously dissolved in solution, it is reasonable to assume

that as long as there is a high energy interface, this type of effect should be observed in fused nanocrystal systems as well. That would suggest that accurate modeling of systems as diverse as geological structures and the high pressure stability of materials would require a knowledge not only of the types of compounds involved, but of their domain size, provided the domains are not greater than nm dimension.

5. Conclusions

In this paper we have presented Se EXAFS data obtained on 2.7 nm radius CdSe nanocrystals above and below the observed solid-solid phase transition. The low pressure wurtzite phase data can be fit with the Murnaghan equations of state to yield a value of B_o = 37 ± 6 GPa and B_o' = 11 ± 3. The high pressure phase EXAFS data is in good agreement with a bulk rock salt structure. Despite this fact, the phase transition does not occur until the system has been pressurized 3.5 GPa above the bulk limit of stability. This elevation in phase transition pressure can be modeled in terms of surface thermodynamics where the excess PdV work put into the system is required to balance a higher surface energy in the high pressure phase. A value of the high pressure phase surface tension can be calculated and is found to be 1.9 N/m in comparison with a value of 0.9 N/m in the low pressure phase. The dependence of the phase transition pressure on nanocrystal size will be used to test the validity of this construction. It appears that dynamical effects associated with limiting the maximum possible fluctuation length are not as important as surface energy effects.

6. Acknowledgements

The authors acknowledge Andreas Kadavanich for his help in collecting the EXAFS data presented here. APA wishes to acknowledge an Alfred P. Sloan Foundation Fellowship. This work has been partially supported by the donors of the Petroleum Research Fund, administered by the American Chemical Society; and by the Director, Office of Energy Research, Office of Basic Energy Sciences, Materials Sciences Division, of the U.S. Department of Energy under Contract No. DE-AC03-76SF00098. These experiments were performed using the facilities of the University of California - Lawrence Livermore National Lab PRT at the Stanford Synchrotron Radiation Laboratory, which is operated by the Department of Energy, Division of Chemical Sciences. The SSRL Biotechnology Program is supported by the NIH, Biomedical Resource Technology Program, Division of Research Resources.

7. References

1. Haase, M. and Alivisatos, A.P.: J. Phys. Chem. **96**, 6756 (1992).

2. Zhao, X.S., Schroeder, J., Persans, P.D., and Bilodeau, T.G.: Phys. Rev. B. **43**, 12580 (1991).

3. Tolbert, S.H. and Alivisatos, A.P: Zeitschrift fur Physik D - Atoms, Molecules, and Clusters. In press.

4. Alivisatos, A.P., Harris, T.D., Brus, L.E., and Jayaraman, A.: J. Chem. Phys. **89**, 5979 (1988).

5. Edwards, A.L. and Drickamer, H.G.: Phys. Rev. **122**, 3196 (1962).

6. Zhao, X.-S., Schroeder, J., Bilodeau, T.G., and Hwa, L.-G.: Phs. Rev. B. **40**, 1257 (1989).

7. Onodera, A.: Rev. Phys. Chem. Japan **39**, 65 (1969).

8. Cui, L.J., Venkateswaran, U.D., and Weinstein, B.A.: Phys. Rev. B. **45**, 9248 (1992).

9. Coombes, C.J.: J. Phys. F **441** (1972).

10. Buffat, P. and Borel, J.-P.: Phys. Rev. A **13**, 2287 (1976).

11. Goldstein, A.N., Echer, C.M., and Alivisatos, A.P.: Science **256**, 1425 (1992).

12. Murray, C.B., Norris, D.J., and Bawendi, M.G.: J. Am. Chem. Soc., in press.

13. Ingalls, R., Crozier, E.D., Whitmore, J.E., Seary, A.J. and Tranquada, J.M.: J. Appl. Phys. **51**, 6 (1980).

14. Teo, B.K. *EXAFS: Basic Principles and Data Analysis*, Springer-Verlag, Berlin, 1986, pp. 21-52.

15. Pankove, J.I. *Optical Processes in Semiconductors*, Dover Publications Inc., New York, 1971, pp. 1-21.

16. Froyen, S. and Cohen, M.L.: Phys. Rev. B **28**, 3258 (1983).

17. Cline, C.F. and Douglas, R.S.: J. Appl. Phys. **36**, 2869 (1965).

18. Hanneman, R.E., Danus, M.D., and Gatos, H.C.: J. Phys. Chem. Solids **25**, 293 (1964).

19. Murnaghan, F.D.: Proc. Natl. Acad. Sci. USA **30**, 224, (1944).

20. Mariano, A.N. and Warekois, E.P.: Science **142**, 672 (1963).

DATE
FILMED
1/21/94
END